ISSN (Print) 1226-1750
ISSN (Online) 2233-6656
Journal of Magnetics 24(1), 135-141 (2019) https://doi.org/10.4283/JMAG.2019.24.1.135

Novel Rotor Winding Investigation for Reduction of Torque Pulsation and Electromagnetic Noise in Squirrel Cage Induction Motor

Yang Zhou[1]*, Xiaohua Bao[1], Wuhua Jiang[2], Jiwei Liu[1], and Wei Xu[1]

[1]*School of Electrical Engineering and Automation, Hefei University of Technology, Hefei, Anhui, China*
[2]*School of Traffic and Transportation Engineering, Hefei University of Technology, Hefei, Anhui, China*

(Received 28 June 2018, Received in final form 14 December 2018, Accepted 21 January 2019)

In the design of squirrel-cage induction machines, torque pulsation and electromagnetic noise always exist. However, they cannot be minimized simultaneously with no matter which slot combination. Electromagnetic noise is aroused by the spatial harmonics in the air gap which are generated by stator magneto-motive force and rotor magneto-motive force. Generally, stator slot number cannot be changed while rotor slot number and slot size could be modified optionally. One set of uniform-bar rotor winding cannot solve this problem. To investigate this issue, this paper proposes a novel rotor winding connection topology for the simultaneous reduction of torque pulsation and electromagnetic noise. 2D finite element models with conventional rotor winding and novel rotor winding are simulated and compared.

Keywords : squirrel-cage induction machine, rotor winding, electromagnetic noise, torque pulsation

1. Introduction

Designs with low torque pulsation and low electromagnetic noise are pursued by motor designers. When the motor is in operation, there are interactions between fundamental magneto-motive force (MMF) and harmonic MMFs of stator and rotor. Low-order radial force produced on the inner surface of stator and rotor is varying with time and space which is the main source of electromagnetic noise.

Many papers are contributed for the enhancement of low torque pulsation or low electromagnetic noise in electric machines. Integer slot winding and fractional slot winding type machines are investigated and compared on torque ripples in interior permanent magnet machine [1]. Fractional slot winding type machine compared to conventional integer slot winding shows low cogging-torque. Slot combinations [2, 3] in induction machines are investigated and electromagnetic noises of different slot combinations are analyzed. Pole and slot combination [4-7] in permanent magnet synchronous machines is studied. A lot of work are done in the reduction of torque pulsation. Besides, in the aspects of reducing electromagnetic noise, in the design of small-scale motor, skewed rotor is often adopted for the reduction of electromagnetic noise. Many papers [8-10] are dedicated to the investigation of skewed rotor and dual skewed rotor as well.

According to the previous research, a slot combination with low-order slot harmonic has low torque pulsation but electromagnetic noise is very large. Another slot combination with high-order slot harmonic has high torque pulsation but electromagnetic noise is very small. Conventional slot combination is powerless to balance these two targets. This paper proposes a novel two-end-ring rotor winding structure (which is the combination of two different kinds of slot combinations) for the balance of torque pulsation and electromagnetic noise in squirrel-cage induction motor. Different conventional slot combinations and novel rotor winding structure are analyzed and compared.

2. Theoretical Analysis

In the selection of number of rotor slots for squirrel-cage induction motor, there should be appropriate cooperation between number of stator slots and number of rotor slots which is usually called slot combination. If combi-

*Corresponding author: Tel: +86-0551-62905883
Fax: +86-0551-62905883, e-mail: sukz@ustc.edu

This paper was presented at the IcAUMS2018, Jeju, Korea, June 3-7, 2018.

nation is improper, this may lead to deterioration of motor performance, for instance, additional loss, additional torque, vibration and noise may increase so that makes efficiency decline, temperature rise, starting performance worsen and unable to start up if serious.

2.1. Effect of slot combination on additional loss

Additional loss of induction motor is mainly caused by air gap harmonic fluxes. These harmonic fluxes produce high frequency iron-core loss (surface loss & tooth pulsation loss) in iron core of stator and rotor; Besides, high frequency current loss in cage bars is produced. Among these, slot harmonic flux of stator and rotor is of most influence.

While slot numbers of stator and rotor are equal, the case of induced potential in rotor bars by stator slot harmonic magnetic flux is presented in Fig. 1. It can be seen that induced potentials (by stator slot harmonic magnetic flux) of adjacent bars are equal in size and identical in phase. Hence, there is no high frequency current loss (including transverse current loss) produced in rotor bars under equal-slots combination. While slot numbers of stator and rotor are close, top width of rotor tooth has tiny difference with wave length of stator slot harmonics. So tooth pulsation loss will be small under the case. In terms of reduction of additional loss, slot numbers of stator and rotor should be as close as possible.

2.2. Effect of slot combination on asynchronous additional torque

In the magnetic field generated by stator winding of three phase induction motor, there are a series of harmonics which have different pole numbers and rotate with various speeds and directions. Similar to the case of asynchronous main torque generated by the fundamental magnetic field, stator harmonic magnetic field could induce current in rotor cage and produces a harmonic magnetic field with the same pole number, speed and rotating direction. The torque generated by the interaction of these two magnetic fields is called asynchronous additional torque. It reduces the value of minimum torque, influences the rising stability at start-up. Motor could prowl at low speed and could not reach normal speed if serious.

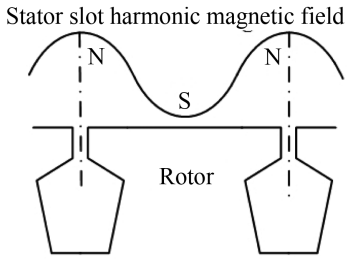

Fig. 1.

When slot numbers of stator and rotor are close, induced current by stator slot harmonics in rotor bars is relatively small. Hence, asynchronous additional torque is small.

When vp/Z_2 is larger than 0.8, asynchronous additional torque will be very tiny. Because stator slot harmonic ($v = Z_2/p + 1$) is the most harmful, for limitation of asynchronous additional torque, slot number of rotor should follow (1) and (2).

$$\frac{vp}{Z_2} = \frac{p\left(\frac{Z_1}{p}+1\right)}{Z_2} \geq 0.8 \tag{1}$$

$$Z_2 \leq 1.25(Z_1 + p) \tag{2}$$

Where : p is pole number

: Z_1, Z_2 are slot numbers of stator and rotor

2.3. Effect of slot combination on synchronous additional torque

When pole numbers and speeds of v_b-th stator harmonic and μ_a-th rotor harmonic induced by v_a-th stator harmonic are the same, these two harmonic magnetic fields will generate synchronous additional torque. Similarly, it would worsen start-up performance of the motor.

Since amplitudes of both stator and rotor slot harmonics are both large, especially for first and second order slot harmonics, the interaction of first, second order slot harmonics of stator and rotor should be avoided in the selection of slot combination. Conditions of producing synchronous additional torque by the interaction of stator and rotor main harmonics are listed below.

1) Interaction of first order slot harmonics of stator and rotor:

$$\begin{cases} Z_2 = Z_1,\ s = 1 \\ Z_2 = Z_1 + 2p,\ s < 1 \\ Z_2 = Z_1 - 2p,\ s > 1 \end{cases} \tag{3}$$

2) Interaction of second order slot harmonics of stator and rotor:

$$\begin{cases} Z_2 = Z_1,\ s = 1 \\ Z_2 = Z_1 + p,\ s < 1 \\ Z_2 = Z_1 - p,\ s > 1 \end{cases} \tag{4}$$

3) Interaction of second order rotor slot harmonic and stator phase harmonic:

$$\begin{cases} Z_2 = 2mpk_1(k_1 > 0),\ s = 1 \\ Z_2 = 2mpk_1 + 2p(k_1 > 0),\ s < 1 \\ Z_2 = 2mpk_1 - 2p(k_1 > 0),\ s > 1 \end{cases} \quad (5)$$

Where : s is slip ration of stator and rotor speed
: m is phase number of stator winding
: k_1 is positive integer

2.4. Effect of slot combination on vibration and noise

Electromagnetic noise is derived from electromagnetic vibration which is motivated by the electromagnetic force produced on steel core by the air gap magnetic field. Moreover, air gap magnetic field is depended on stator, rotor winding excitation magneto-motive force (MMF) and air gap magnetic permeance. So the investigation of electromagnetic noise should be started from these aspects.

There are two components (radial and tangential) of magnetic force generated on stator tooth. The deformation of stator core caused by radial component is the main source of electromagnetic noise; Tangential component corresponds to electromagnetic torque which makes tooth inflection and produces partial deformation. This is a secondary source of electromagnetic noise.

1) Stator MMF and rotor MMF

Air gap compound MMF $f(\theta, t)$ (1) is comprised of fundamental compound MMF $f_p(\theta, t)$, stator harmonic MMF $f_v(\theta, t)$ and rotor harmonic MMF $f_\mu(\theta, t)$. Among these, the expression of each component is presented in (7). When slot number q of each pole and each phase in three-phase stator winding is an integer, harmonic order v of stator MMF equals to (8). Symbol '+' represents the rotation direction is the same as fundamental MMF while symbol '–' represents the rotation direction is opposite to fundamental MMF.

Since slot harmonics in stator MMF will not be weakened using short pitch or distributed winding, they are uppermost origin leading to electromagnetic noise. Harmonic order v_t of slot harmonics is presented in (9). Angular frequency ω_v of v-th harmonic relative to stator core is presented in (10).

For squirrel-cage rotor, there are no phase-zone harmonics due to too much phases. Rotor slot harmonics only exist. Harmonic order μ_t of rotor slot harmonics is presented in (11). Angular frequency $\omega_{\mu t}$ of μ_t-th harmonic relative to stator core is presented in (12).

$$f(\theta,t) = f_p(\theta,t) + \sum_v f_v(\theta,t) + \sum_\mu f_\mu(\theta,t) \quad (6)$$

$$\begin{cases} f_p(\theta,t) = F_p \cos(p\theta - \omega_1 t - \varphi_0) \\ f_v(\theta,t) = F_v \cos(v\theta - \omega_1 t - \varphi_v) \\ f_\mu(\theta,t) = F_\mu \cos(\mu\theta - \omega_1 t - \varphi_\mu) \end{cases} \quad (7)$$

$$v = (6k_1 + 1)p, \quad k_1 = \pm 1, \pm 2, \pm 3, \cdots \quad (8)$$

$$v_t = \left(k_1 \frac{Z_1}{p} + 1\right)p = k_1 Z_1 + p, \quad k_1 = \pm 1, \pm 2, \pm 3, \cdots \quad (9)$$

$$\omega_v = \omega_1 \quad (10)$$

$$\mu_t = k_2 Z_2 + p, \quad k_2 = \pm 1, \pm 2, \pm 3, \cdots \quad (11)$$

$$\omega_{\mu t} = \omega_1 \left[1 + k_2 \frac{Z_2}{p}(1 - s)\right] \quad (12)$$

Where : θ is mechanical angular displacement.
: t is time.
: F_p is amplitude of fundamental compound MMF.
: F_v is amplitude of stator v-th harmonic MMF.
: F_μ is amplitude of rotor μ-th harmonic MMF.
: p is pole pair number of fundamental compound MMF.
: ω_1 is angular frequency of fundamental compound MMF.
: φ_0 is initial phase angle of fundamental compound MMF.
: φ_v is initial phase angle of stator v-th harmonic MMF.
: φ_μ is initial phase angle of rotor μ-th harmonic MMF.

2) Air gap magnetic permeance

Assume that stator has slots and rotor has smooth surface, then main component of air gap magnetic permeance can be expressed as (13).

Assume that stator has smooth surface and rotor has slots, rotor rotating at speed n, then main component of air gap magnetic permeance can be expressed as (14).

Actually, stator and rotor of induction machine both have slots, so air gap magnetic permeance (15) is deduced according to (13) and (14). Among these, Λ_0 is constant part of air gap magnetic permeance, Λ_1 is first-order stator slot harmonic's amplitude of air gap magnetic permeance, Λ_2 is first-order rotor slot harmonic's amplitude of air gap magnetic permeance. $\Omega_2 = 2\pi n/60$ is rotor mechanical angular speed.

$$\Lambda(\theta) = \Lambda_0 + \Lambda_1 \cos Z_1\theta = \Lambda_0\left(1 + \frac{\Lambda_1}{\Lambda_0}\cos Z_1\theta\right) \quad (13)$$

$$\begin{aligned} \Lambda(\theta,t) &= \Lambda_0 + \Lambda_2 \cos Z_2(\theta - \Omega_2 t) \\ &= \Lambda_0\left\{1 + \frac{\Lambda_2}{\Lambda_0}\cos Z_2\left[\theta - \frac{\omega_1}{p}(1-s)t\right]\right\} \end{aligned} \quad (14)$$

$$\begin{aligned} \Lambda(\theta,t) &= \Lambda_0\left(1 + \frac{\Lambda_1}{\Lambda_0}\cos Z_1\theta\right)\left\{1 + \frac{\Lambda_2}{\Lambda_0}\cos Z_2\left[\theta - \frac{\omega_1}{p}(1-s)t\right]\right\} \\ &\approx \Lambda_0 + \Lambda_1 \cos Z_1\theta + \Lambda_2 \cos Z_2\left[\theta - \frac{\omega_1}{p}(1-s)t\right] \end{aligned} \quad (15)$$

3) Air gap magnetic field

When magnetic reluctance of steel core is ignored, instantaneous value of air gap flux density is expressed as (16). For simplification, there are five terms without consideration of minor components. Expression (17) is about fundamental magnetic field. Expression (18) is harmonic magnetic field of stator winding. Expression (19) is harmonic magnetic field of cage rotor. Expression (20) is first-order harmonic magnetic field of stator air-gap magnetic permeance. Expression (21) is first-order harmonic magnetic field of rotor air-gap magnetic permeance.

$$b(\theta,t)=f(\theta,t)\cdot\Lambda(\theta,t)=\left[f_p(\theta,t)+\sum_v f_v(\theta,t)+\sum_\mu f_\mu(\theta,t)\right]\Lambda(\theta,t) \tag{16}$$

$$b_1=f_p(\theta,t)\cdot\Lambda_0=B_1\cos(p\theta-\omega_1 t-\varphi_0) \tag{17}$$

$$b_v=f_v(\theta,t)\cdot\Lambda_0=B_v\cos(v\theta-\omega_1 t-\varphi_v) \tag{18}$$

$$b_\mu=f_\mu(\theta,t)\cdot\Lambda_0=B_\mu\cos(\mu\theta-\omega_1 t-\varphi_\mu) \tag{19}$$

$$b_{01}^{(1)}=f_p(\theta,t)\cdot\Lambda_1\cos Z_1\theta=B_{01}^{(1)}\cos\left[(Z_1+p)\theta-\omega_1 t-\varphi_0\right]+B_{01}^{(1)}\cos\left[(-Z_1+p)\theta-\omega_1 t-\varphi_0\right] \tag{20}$$

$$b_{02}^{(1)}=f_p(\theta,t)\cdot\Lambda_2\cos Z_2\left[\theta-\frac{\omega_1}{p}(1-s)t\right]=B_{02}^{(1)}\cos\left[(Z_1+p)\theta-\omega_\mu t-\varphi_0\right]+B_{02}^{(1)}\cos\left[(-Z_1+p)\theta-\omega_\mu t-\varphi_0\right] \tag{21}$$

4) Radial force

There are a series of interactions between stator's and rotor's magnetic field existing in the air gap which could produce many electromagnetic forces. According to Maxwell's law, radial electromagnetic force (per unit area) in the air gap between stator and rotor can be expressed by (22). Among these, $b(\theta, t)$ is air gap flux density and μ_0 is magnetic permeability of air.

$$p_r=\frac{b^2(\theta,t)}{2\mu_0} \tag{22}$$

In the view of noise and vibration, main forces are discussed below:

a. Force produced by fundamental wave

Force produced by fundamental wave is presented in (23) which is divided into two parts. p_0 (24) is the constant part of radial force and p_1 (25) is the alternating part of radial force.

$$p_r=\frac{b_1^2}{2\mu_0}=\frac{1}{2}\frac{B_1^2}{2\mu_0}\left[1+\cos 2(p\theta-\omega_1 t-\varphi_0)\right]=p_0+p_1 \tag{23}$$

$$p_0=\frac{B_1^2}{4\mu_0} \tag{24}$$

$$p_1=\frac{B_1^2}{4\mu_0}\cos(2p\theta-2\omega_1 t-2\varphi_0) \tag{25}$$

b. Force produced by stator and rotor harmonic MMFs

Force produced by stator and rotor harmonic MMFs is presented in (26). For generating electromagnetic noise, the term $2b_\nu b_\mu$ in (26) is much more important. b_ν^2 and b_μ^2 are ignored here and substitute (18) and (19) in (26) which acquires (27). In the formula, $r = \mu \pm \nu$ is spatial order. On one hand, noise and vibration generated by electromagnetic force is related with the amplitude of the force; On the other hand, it is related with the order of the force. The lower the order, the bigger the noise. Usually amplitude of the vibration in steel core is about inversely proportional to r^4. So low-order force is the main research point.

$$p_{\nu\mu}=\frac{(b_\nu+b_\mu)^2}{2\mu_0}=\frac{b_\nu^2+2b_\nu b_\mu+b_\mu^2}{2\mu_0} \tag{26}$$

$$p_{\nu\mu}=\frac{B_\nu B_\mu}{2\mu_0}\cos[(\mu\pm\nu)\theta-(\omega_\mu\pm\omega_1)t-(\varphi_\mu\pm\varphi_\nu)] \tag{27}$$

When in consideration of first order slot harmonics of stator and rotor MMF, frequency of the force is presented as (28). Due to $Z_2/p >> 2$ and s of induction machines is very small, two cases in (28) could be unified as (29). It is obvious to see that frequency of the most prominent harmonic MMF (first-order slot harmonics) depends on rotor slot number Z_2. But order r of the force depends on the difference of stator slots and rotor slots. This is conflicting with adopting close slot combination for reduction of stray loss. Hence, it should be taken into full consideration in the selection of slot number.

Ignored two terms b_ν^2 and b_μ^2 in (26) represent stator and rotor harmonic magnetic field which produce twice power frequency ($2f_1$) force. Since the frequency is very low, it makes little impact on the total noise. Furthermore, the order of these two terms are 2ν and 2μ which are very high, the noise caused is very little.

$$\begin{cases}\mu_t\cdot\nu_t>0 \quad \& \quad r=\mu_t-\nu_t \\ f_r'=\dfrac{\omega_{\mu t}-\omega_1}{2\pi}=\dfrac{\omega_1+\frac{Z_2\omega_1}{p}(1-s)-\omega_1}{2\pi}=\dfrac{Z_2\omega_1}{p}(1-s)f_1 \\ \mu_t\cdot\nu_t<0 \quad \& \quad r=\mu_t+\nu_t \\ f_r''=\dfrac{\omega_{\mu t}+\omega_1}{2\pi}=\dfrac{\omega_1+\frac{Z_2\omega_1}{p}(1-s)+\omega_1}{2\pi}=\left[\dfrac{Z_2\omega_1}{p}(1-s)+2\right]f_1\end{cases} \tag{28}$$

$$f_r = f_r' = f_r'' = \frac{Z_2}{p} f_1 \tag{29}$$

c. Force produced by 1st slot harmonics of stator and rotor air-gap magnetic permeance

According to (20) and (21), the possible order leading to vibration could be (30). This states that it is relevant to stator slot number Z_1 and rotor slot number Z_2. To avoid large electromagnetic vibration and noise, low orders r = 0, ± 1, ± 2, ± 3 (31) should not appear in the selection of slot combination. Since vibration amplitude caused by higher order of the force is very small, it could be ignored in common induction machines.

$$r = (\pm Z_2 + p) \pm (\pm Z_1 + p) \tag{30}$$

$$\begin{cases} Z_2 = Z_1 \pm i \\ Z_2 = Z_1 \pm 2p \pm i \end{cases} \quad (i = 0, 1, 2, 3) \tag{31}$$

3. Simulation

In the design of a squirrel-cage induction motor, torque pulsation and electromagnetic noise are ambivalent. When torque pulsation is low at a certain slot combination, electromagnetic force order will be small but electromagnetic noise is large, vice versa.

To specify this statement, a 6-pole (36 stator slots) machine is selected as the investigation object, specified parameters of the motor is listed in Table 1. In consideration of balance of torque pulsation and electromagnetic noise, a novel two-end-ring structure is proposed as seen in Fig. 2(b). Different from conventional structure in Fig. 2(a), torque pulsation and electromagnetic noise could be reduced and balanced by the optimization of parameter h and h_s. According to the characteristic of magnetic path, closed-slot depth h determines the proportion of 7-slot cage rotor winding. Its effect becomes greater when its value becomes smaller. That's to say, when the value h is small, the proposed two-end-ring rotor winding tends to be like 35-slot rotor winding in the paper. Correspondingly, the torque pulsation is relatively low but electromagnetic noise is large; When the value h is large, the proposed two-end-ring rotor winding tends to be like 28-slot rotor winding in the paper. Correspondingly, the torque pulsation is relatively high but electromagnetic noise is low. The value of h_s is inferred to the rotor

Table 1. Main parameters of simulated induction motor.

Parameters	Simulated motor
Rated power	5.5 kW
Rated voltage	380 V
Connection	Y
Rated frequency	50 Hz
Slot combination Z_1	36
Number of winding layers	1
Dimensions (mm)	ϕ210ϕ 148ϕ 48ϕ 180
Air gap length	0.35 mm

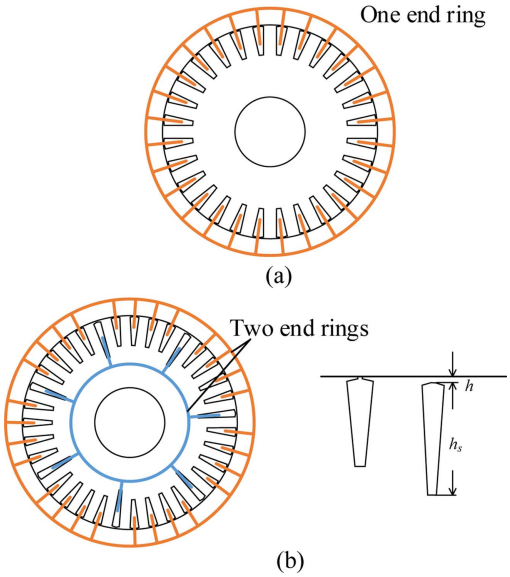

Fig. 2. (Color online) (a) Conventional one end ring structure, (b) Proposed two end rings structure.

Table 2. Electromagnetic force order of different slot combinations.

$r=\mu \pm v$	k_1	-1	+ 1	-2	2	-3	3	-4	4
k_2	v / μ	-15	21	(-33)	(+39)	-51	57	(-69)	(+75)
-1	-25								
1	31			(-2)					
-2	-53								
2	59								

(a) Z_1=36, Z_2=28

$r=\mu \pm v$	k_1	-1	+ 1	-2	2	-3	3	-4	4
k_2	v / μ	-15	21	(-33)	(+39)	-51	57	(-69)	(+75)
-1	-30			(+3)					
1	36			(+3)	(-3)				
-2	-63								
2	69							0	

(b) Z_1=36, Z_2=33

$r=\mu \pm v$	k_1	-1	+ 1	-2	2	-3	3	-4	4
k_2	v / μ	-15	21	(-33)	(+39)	-51	57	(-69)	(+75)
-1	-32			(+1)					
1	38			5	(-1)				
-2	-67							2	
2	73							4	-2

(c) Z_1=36, Z_2=35

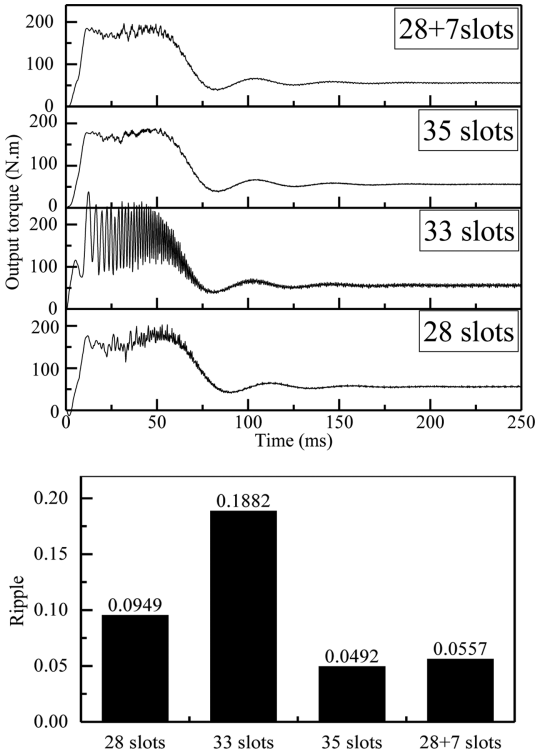

Fig. 3. Output torque and torque ripple at steady state of different slot combinations.

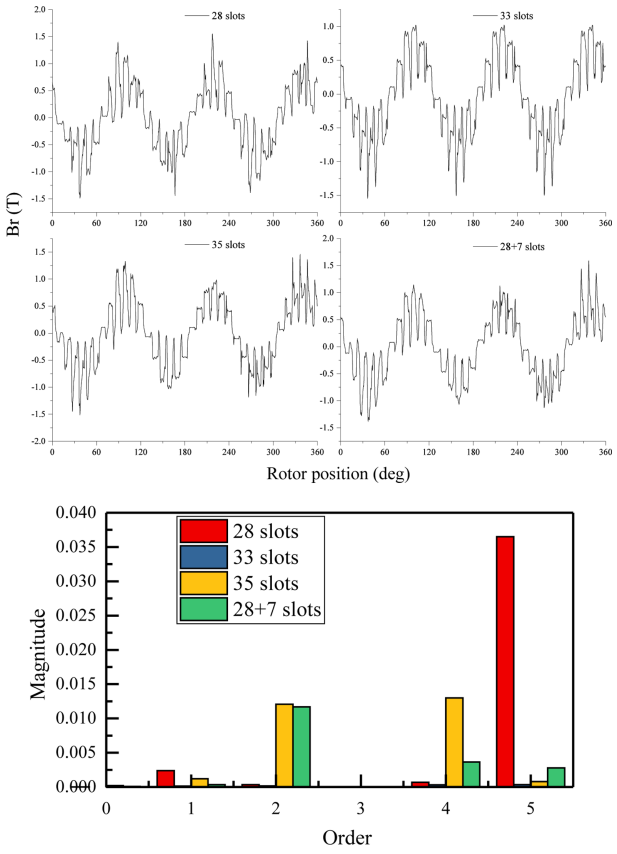

Fig. 4. (Color online) Radial air-gap flux density at circumferential position and its spatial spectrum.

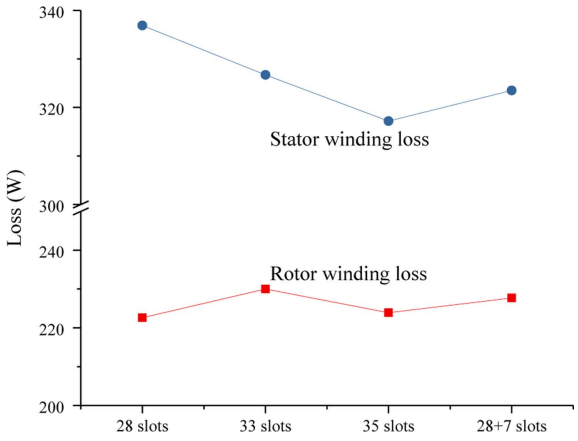

Fig. 5. (Color online) Main losses of different slot combinations.

resistance and rotor yoke magnetic flux density. The effect of value h_s is the same as value h. The purpose of adopting two-end-ring rotor winding structure is to find the balanced point of 28-slot rotor winding and 35-slot rotor winding.

Table 2 gives electromagnetic force order of several slot combinations. Among these, brackets in the table represent slot harmonics. First-order slot harmonics are the main concern. It could be seen in Table 2 that the lowest order of Z_2 = 28, 33, 35 is 2, 3 and 1 respectively. Fig. 3 gives the output torque and torque ripple at rated load. Torque ripple refers to the ratio of the peak to peak-to-average.

It could be seen in Fig. 3 that torque ripple gets larger with order. Especially, torque pulsation at startup is very large under 36-33 slot combination. As mentioned above, when gap of stator and rotor slots is times of pole pair, unexpected synchronous and asynchronous additional torque will play a significant role.

This paper proposes a structure of two end rings (28 slots connected, 7 slots connected). Through optimization, h = 0.5 mm and h_s = 18 mm. The slot width is the same as 36-35 slot combination. Fig. 4 gives radial flux density at rotor position of different slot structures and its spatial harmonics spectrum. Among these, third order is the main order which is not the research point and not displayed in Fig. 4. Since noise level of higher order is very small, only 5th below orders are presented. It can be seen that the proposed 28+7 slots structure has quite lower amplitude at low orders compared with conventional 36-35 slot combination. However, the torque pulsation increases a little. Lastly, main losses of different slot combinations as seen in Fig. 5 are compared. Winding losses of close slot combinations have a little difference.

Through the comparison as seen in Fig. 3, 4 and 5, the proposed two-rotor-winding structure has good balance of torque pulsation and electromagnetic noise compared with conventional one-rotor-winding structure.

4. Conclusions

This paper proposes a two-end-ring rotor winding structure for the balance of torque pulsation and electromagnetic noise in squirrel-cage induction motor. Through the comparison with conventional (one end ring) slot combination, the proposed structure has lower spatial harmonics and electromagnetic noise but torque pulsation increases very little. What's more, stator and rotor winding losses do not change much. It is useful and interesting for the minimization of torque pulsation and noise level in squirrel-cage induction machines with two sets of rotor winding.

Acknowledgments

This work was supported by the National Science Funds of China (No. 51677051 and No. 51377039), Anhui Province key laboratory of Large-scale Submersible Electric Pump and Accoutrements.

References

[1] J. Seo, J. Magn. **18**, 3 (2013).
[2] Y. Dai, Q. F. Zhang, L. W. Song, and S. M. Cui, Proc. CSEE **30**, 27 (2010).
[3] X. F. Huo, G. Li, and X. Li, Theory. Design, **2** (2012).
[4] H. W. Jun, H. S. Seol, and J. Lee, IEEE Trans. Magn. **53**, 11 (2017).
[5] T. Sun, J. M. Kim, G. H. Lee, J. P. Hong, and M. R. Choi, IEEE Trans. Magn. **47**, 5 (2011).
[6] Ming-Tsan Peng and Tim J. Flack, IEEE Trans. Magn. **52**, 6 (2016).
[7] T. Gundogdu, Z. Q. Zhu, and J. C. Mipo, ICEMS (2017) pp. 1-6.
[8] L. Wang, X. H. Bao, C. Di, Y. Zhou, and Q. F. Lu, IET Elec. Pow. Appl. **11**, 8 (2017).
[9] J. Bao, J. Paulides, K. Boynov, and E. Lomonova, Intermag (2017) pp 1-2.
[10] D. D. Zhang, L. X. Bu, C. Y. He, R. C. An, and T. Wu, IEMDC (2017) pp 1-8.